THE JOURNAL OF BIOLOGICAL CHEMISTRY VOL. 290, NO. 26, pp. 16202–16214, June 26, 2015

FBXO32 Targets c-Myc for Proteasomal Degradation and Inhibits c-Myc Activity*

Received for publication, February 16, 2015, and in revised form, May 4, 2015 Published, JBC Papers in Press, May 5, 2015, DOI 10.1074/jbc.M115.645978

Zhichao Mei[‡], Dawei Zhang[‡], Bo Hu[‡], Jing Wang[‡], Xian Shen[§], and Wuhan Xiao[‡¶1]

From the [‡]Key Laboratory of Aquatic Biodiversity and Conservation and the [¶]State Key Laboratory of Freshwater Ecology and Biotechnology, Institute of Hydrobiology, Chinese Academy of Sciences, Wuhan 430072, China and the [§]First Hospital of Wenzhou Medical University, Wenzhou 325000, China

Background: FBXO32 is an E3 ubiquitin ligase that plays important roles in tumorigenesis and muscle atrophy.
Results: c-Myc was found to be a target of FBXO32 for proteasomal degradation.
Conclusion: FBXO32 targets Lys-326 of c-Myc to form polyubiquitin chains, resulting in inhibition of cell proliferation.
Significance: FBXO32 may mediate c-Myc proteasomal degradation.

FBXO32 (MAFbx/Atrogin-1) is an E3 ubiquitin ligase that is markedly up-regulated in muscle atrophy. Although some data indicate that FBXO32 may play an important role in tumorigenesis, the molecular mechanism of FBXO32 in tumorigenesis has been poorly understood. Here, we present evidence that FBXO32 targets the oncogenic protein c-Myc for ubiquitination and degradation through the proteasome pathway. Phosphorylation of c-Myc at Thr-58 and Ser-62 is dispensable for FBXO32 to induce c-Myc degradation. Mutation of the lysine 326 in c-Myc reduces c-Myc ubiquitination and prevents the c-Myc degradation induced by FBXO32. Furthermore, overexpression of FBXO32 suppresses c-Myc activity and inhibits cell growth, but knockdown of FBXO32 enhances c-Myc activity and promotes cell growth. Finally, we show that *FBXO32* is a direct downstream target of c-Myc, highlighting a negative feedback regulation loop between c-Myc and FBXO32. Thus, FBXO32 may function by targeting c-Myc. This work explains the function of *FBXO32* and highlights its mechanisms in tumorigenesis.

FBXO32 (also known as MAFbx or Atrogin-1) was originally identified as a muscle-specific gene required for muscle atrophy (1, 2). FBXO32 was designated as a muscle-specific E3 ubiquitin ligase because it contains the F-box domain. This is a characteristic of E3 ligases that function as one component of a SCF (Skp1, Cullin, F-box protein) ubiquitin ligase complex (1, 2). FBXO32 lacks leucine-rich repeats or WD40 repeats but it does contain a class II PDZ domain (2), which interacts with specific sequences at the carboxyl terminus of the target proteins (3, 4). In addition, FBXO32 also contains two nuclear localization signals, which suggests that it may target transcription factors or other nuclear proteins for ubiquitination (5).

As an ubiquitin E3 ligase, FBXO32 has been shown to target several proteins for proteasomal degradation (6–8). The two most widely known targets of FBXO32 in skeletal muscle are the initiation factor, eIF3-f, and the myogenic regulatory factor, MyoD. In addition to targeting the proteins mediating FBXO32 function in muscle atrophy, FBXO32 also targets MKPK phosphatase-1 for proteasomal degradation and is probably involved in ischemia/reperfusion-induced cardiomyocyte apoptosis (8).

Some evidence suggests that *FBXO32* might also play an important role in tumorigenesis. The expression level of FBXO32 is closely correlated with the methylation status of the *FBXO32* promoter in ovarian cancer cell lines (9). Restoration of FBXO32 in ovarian cancer cells inhibits colony formation *in vitro* and xenograft tumor growth in athymic nude mice. Moreover, patients with higher *FBXO32* promoter methylation tend to have shorter progression-free survival. This suggests a tumor-suppressive role of *FBXO32* (9). In addition, the FBXO32 expression is also decreased in esophageal squamous cell carcinoma (10). EZH2 supports the survival of alveolar rhabdomyosarcoma by repressing FBXO32 (11), but, up-regulation of FBXO32 is a hallmark of cancer cachexia caused by muscle wasting (12, 13). Therefore, the role of *FBXO32* in tumorigenesis is still unclear, and the underlying mechanism is poorly understood.

c-Myc is a short-lived protein and a classic oncogene regulated at multiple steps. One of the most prominent mechanisms for c-Myc degradation in cells is through the ubiquitin-proteasome pathway (14). As a component of the RING finger domain, ubiquitin ligase complex (15, 16), Fbw7 is the best studied SCF-type E3 ubiquitin ligase for mediating c-Myc degradation. The FBW7 recognizes phosphorylated c-Myc at Thr-58, which is mediated by glycogen synthase kinase 3 (Gsk3) (15, 16). Another RING finger E3 ligase, Skp2, recognizes a conserved sequence element in the amino terminus of c-Myc (MBII) as well as the HLH-LZ motifs (amino acids 367–439). It promotes its polyubiquitination and degradation, resulting in the enhancement of c-Myc transcriptional activity (17, 18). The third RING finger E3 ligase, β-TrCP, binds to the amino terminus of c-Myc and uses the UbcH5 ubiquitin-conjugating enzyme (E2) to form heterotypic polyubiquitin chains on c-Myc. This enhances c-Myc stability (19).

* This work was supported by CAS Major Scientific and Technological Project XDA08010208; NSFC Grants 31461163003, 31071212, and 91019008 (to W. X.); and the Natural Science Foundation of Zhejiang Province Grant 2012C37080 (to X. S.). The authors declare that they have no conflicts of interest with the contents of this article.
[1] To whom correspondence should be addressed: Institute of Hydrobiology, Chinese Academy of Sciences, Wuhan 430072, China. Tel.: 87-27-68780087; Fax: 86-27-68780087; E-mail: w-xiao@ihb.ac.cn.

Importantly, the expression pattern of FBXO32 is inversely correlated with c-Myc expression during starvation treatment (2). Serum stimulation induces expression of c-Myc immediately (20, 21), but removal of growth factors at any point in the cell cycle results in down-regulation of the c-Myc (22, 23). In contrast, IGF-1 inhibits the transcription of *FBXO32* through the PI3K/Akt/FOXO pathway and blocks dexamethasone-induced atrophy (24); food deprivation increases FBXO32 expression and results in rapid muscle wasting (2). Moreover, activation of FOXO3a leads to a considerable reduction in c-Myc (25, 26).

Given that *FBXO32* is a direct target of FOXO3a (27), we sought to determine whether FBXO32 participates in the degradation of c-Myc. In this study, we identify c-Myc as a substrate of FBXO32 E3 ubiquitin ligase. FBXO32 targets c-Myc for ubiquitination and degradation through the proteasome pathway. Mutation of the lysine 326 in c-Myc reduces c-Myc ubiquitination and prevents c-Myc degradation induced by FBXO32. Moreover, overexpression of FBXO32 suppresses c-Myc activity and inhibits cell growth. In addition, we reveal that FBXO32 is a direct downstream target of c-Myc.

Experimental Procedures

Cell Culture and Transfection—HEK293T, HCT116, A673, and SKOV3 cells were originally obtained from ATCC. HEK293T, HCT116, and A673 cells were maintained in Dulbecco's modified Eagle's medium (DMEM; HyClone) with 10% fetal bovine serum (FBS; HyClone) in 5% CO_2 at 37 °C, whereas SKOV3 cells were maintained in McCoy's 5A medium. VigoFect (Vigorous Biotech, Beijing) was used for cell transfection following the protocol provided by the manufacturer.

Plasmid Constructs—The original wild-type c-Myc and its domain constructs were kindly provided by Stephen Hann. HA-tagged c-Myc(P57S) and c-Myc(T58A) were kindly provided by Scott Lowe. The original *Gadd45α* promoter luciferase reporter was provided by Linda Penn. The pGL3-*E2F2* promoter luciferase reporter was constructed by PCR amplification (28). pGL3-*E2F2*-mut promoter luciferase reporter was constructed by mutating three E-boxes in the promoter (the sequence information will be provided upon requested). The *FBXO32* coding sequence was amplified from cDNA derived from 293T cell total RNA by PCR with the primers 5′-CCCGAATTCGGATGCCATTCCTCGGGCAGGAC-3′ (forward) and 5′-CCCGGTACCTCAGAACTTGAACAAGTTGATAAAG-3′ (reverse) and then subcloned into pCMV-HA vector (Clontech). Phage-CMV-MCS-IZsGreen was used as a retroviral expression vector. FBXO32-WT, FBXO32-ΔF-box, c-Myc-WT, and c-Myc-K326R were subcloned into phage-CMV-MCS-IZsGreen and confirmed by sequencing.

The *FBXO32* promoter (positions −452 to +24) for its luciferase reporter construct was amplified from total DNA extracted from 293T cells by PCR with the primers 5′-CCCCTCGAGGGCTGATCTGGCTGCGGAGGTCG-3′ (forward) and 5′-CCCAAGCTTAGCGTTGCAGGCTCCGGGAGTGC-3′ (reverse). The promoter was then subcloned into pGL4.10 vector (Promega).

For RNA interference experiments, pSuper and lentivirus vector LentiLox3.7 were used to make short hairpin RNA (shRNA) constructs. The target sequence for both pSuper-FBXO32-shRNA-1 and pll3.7-FBXO32-shRNA-1 was 5′-GTCACATCCTTTCCTGGAA-3′. The target sequence for both pSuper-FBXO32-shRNA-2 and pll3.7-FBXO32-shRNA-2 was 5′-GGAAGAAGATGTATTTCAA-3′. pSuper-c-Myc-shRNA-1 and pSuper-c-Myc-shRNA-2 were constructed using the following targeting sequences: 5′- CTATGACCTCGACTACGAC-3′ (pSuper-c-Myc-shRNA-1) and 5′-GACGAGAACAGTTGAAACA-3′ (pSuper-c-Myc-shRNA-2), respectively. The target sequence for pll3.7-c-Myc-shRNA was 5′-GCCATAATGTAAACTGCCT-3′, which targets 5′-UTR of human c-Myc.

For rescue experiments, the cDNA sequence of *FBXO32* corresponding to the target sequence of *FBXO32*-shRNA-2, 5′-GGAAGAAGATGTATTTCAA-3′ (the mutated sites are underlined), was mutated to 5′-GGAAAAAAATGTACTTTAA-3′ (the mutated sites are underlined).

Antibodies and Reagents—The antibodies used were as follows: anti-FBXO32 antibody (7721-1, Epitomics; PAB15627, Abnovo), anti-c-Myc antibody (9E10, Santa Cruz Biotechnology, Inc.; A0309, ABclonal; D84C12, Cell Signaling), anti-E2F2 antibody (6848-1, Epitomics), anti-FLAG antibody (F1804, Sigma-Aldrich), anti-HA antibody (Covance), anti-GAPDH antibody (SC-47724, Santa Cruz Biotechnology), anti-tubulin antibody (EPR1333, Epitomics), and anti-GFP antibody (AG281-1, Beyotime). The reagents used were as follows: MG132 (Calbiochem) and cycloheximide (Sigma-Aldrich).

Semiquantitative Real-time RT-PCR—Total RNA was extracted from cells by using TRIzol reagent (Invitrogen), and cDNA was synthesized using a first-strand cDNA synthesis kit (Fermentas) following the manufacturer's instructions. Human *FBXO32*, *E2F2*, and *Gadd45α* cDNA were amplified with the following primer sequence: *FBXO32*, 5′-AAGTCTGTGCTGGTCGGGAA-3′ (forward) and 5′-AGTGAAGGTGAGGCCTTTGAAG-3′ (reverse); *E2F2*, 5′-GGCCAAGAACAACATCCAGT-3′ (forward) and 5′-TGTCCTCAGTCAGGTGCTTG-3′ (reverse); *Gadd45α*, 5′-ATGACTTTGGAGGAATTCTCG-3′ (forward) and 5′-CATTGATCCATGTAGCGACTT-3′ (reverse). 18S rRNA was used as an internal control. The primers for 18S rRNA were 5′-TCAACTTCGATGGTAGTCGCCGT-3′, and 5′-TCCTTGGATGTGGTAGCCGTTCT-3′.

Luciferase Reporter Assays—HEK293T or HCT116 cells were seeded in 24-well plates and transfected with the indicated plasmids by VigoFect (Vigorous Biotech, Beijing). The pRL-SV40 luciferase reporter (Promega) was included in all transfections for normalization. Luciferase activities were measured 24 h after transfection using the Dual-Luciferase reporter assay system (Promega). Data were normalized to *Renilla* luciferase. Data are reported as the means ± S.E. of three independent experiments performed in triplicate. The statistical analysis was performed using GraphPad Prism version 5 (unpaired Student's *t* test) (GraphPad Software Inc.).

Colony Formation Assays—The stable transfected SKOV3 cells via lentivirus infection were seeded in 6-well plates at 4×10^3 cells/well and cultured in DMEM containing 10% fetal bovine serum for 14 days. The colonies were fixed and stained with 0.4% crystal violet in 50% methanol for 30 min. Dishes were rinsed with water and left for drying at room temperature. Colonies were photographed with a stereomicroscope and counted by ImageJ

software. Only the colonies containing more than 50 cells were set for counting. Data are reported as the means ± S.E. of three independent experiments performed in triplicate. The statistical analysis was performed using GraphPad Prism version 5 (unpaired Student's *t* test) (GraphPad Software Inc.).

ChIP Assays—ChIP assays were performed in HCT116 cells following the protocol described previously (29). The primers for amplifying *FBXO32* promoter were 5′-AGCACCGCTTC-AAGTTTCCACCG-3′ (forward) and 5′-GGCAGTAGCT-GCCGCAGTATTTATCCC-3′ (reverse); the primers for amplifying β-actin promoter were 5′-CAGGGCGTGATGGT-GGGCA-3′ (forward) and 5′-CAAACATGATCTGGGTCAT-CTTCTC-3′ (reverse).

In Vivo Ubiquitination Assays—HEK293T cells were co-transfected with the indicated plasmids using Vigofect. After transfection for 24 h, the cells were collected, lysed, and subjected to immunoprecipitation by Ni^{2+}-nitrilotriacetic acid beads (Novagen) and then examined by Western blotting using anti-HA antibody. The ubiquitin mutants have been described previously (30).

Lentivirus Package—Lentiviruses for gene overexpression were generated by transfecting HEK293T cells with combinations of transducing vector and two packaging vectors, PSPAX2 and pMD2.G. For lentiviral shRNA production, transducing vector was co-transfected with three packaging vectors, PMDLg/pRRE, VSVG, and RSV-Rev, in HEK293T cells. After transfection for 6 h, the medium was replaced with fresh DMEM with 10% FBS. 48 h later, the medium containing the lentivirus particles was harvested, filtered, and transduced into target cells or frozen at −70 °C for subsequent using. Polybrene (8 μg/ml) was added to the medium for improving infection efficiency.

Co-immunoprecipitation and Western Blot Analysis—For Western blot analysis and co-immunoprecipitation, the experimental procedures have been described previously (31). Anti-HA antibody and anti-FLAG antibody-conjugated agarose beads were purchased from Sigma-Aldrich. Protein A/G-Sepharose beads were purchased from GE Healthcare. Glutathione *S*-transferase (GST)-Bind resin was purchased from Novogen. For endogenous immunoprecipitation, the mouse leg muscle was used for extracting protein. The Fuji Film LAS4000 miniluminescent image analyzer system was used to photograph the blots. Multi Gauge version 3.0 was used for quantifying the protein levels based on the band density obtained in Western blot analysis.

Statistical Analysis—Data are presented as mean ± S.E. of three independent experiments performed in triplicate; the statistical analysis was performed using GraphPad Prism version 5.0 (unpaired Student's *t* tests).

Results

FBXO32 Promotes c-Myc Degradation—To study the relationship between FBXO32 and c-Myc, we first transfected HEK293T cells with an equal amount of HA-c-Myc and increasing amounts of HA-FBXO32. Ectopic expression of FBXO32 degraded c-Myc in a dose-dependent fashion (Fig. 1*A*). In contrast, knockdown of endogenous FBXO32 by transiently transfected pSuper-shRNA-1 or pSuper-shRNA-2 in HCT116 cells caused endogenous c-Myc to increase (*first line* from the *top* to the *bottom* in the *left panel* of Fig. 1*B*). Consistently, E2F2, a well defined downstream target of c-Myc, also increased (*second line* from the *top* to the *bottom* in the *left panel* of Fig. 1*B*). The efficiency of pSuper-*FBXO32*-shRNA-1- or pSuper-*FBXO32*-shRNA-2-mediated FBXO32 knockdown was confirmed (*third line* from the *top* to the *bottom* in the *left panel* of Fig. 1*B*). To verify the specificity of *FBXO32*-shRNA-2-mediated FBXO32 knockdown, we performed a rescue experiment. As shown in Fig. 1*C*, overexpression of *FBXO32*-shRNA-2-resistant FBXO32 in HCT116 cells neutralized the effect of *FBXO32*-shRNA-2-mediated c-Myc up-regulation. To determine whether FBXO32-mediated c-Myc reduction was due to FBXO32-induced c-Myc instability, we added the new protein synthesis inhibitor, cycloheximide (CHX)[2] and examined the protein levels at different time points. Without ectopically expressed FBXO32, the overexpressed c-Myc gradually degraded (*left panel* in Fig. 1*D*). However, co-expression of wild-type FBXO32 caused c-Myc to degrade more rapidly (*middle panel* in Fig. 1*D*). In contrast, co-expression of the F-box domain-deleted mutant of FBXO32 obviously prolonged the half-life of c-Myc (*right panel* in Fig. 1*D*). It appears that the mutant, FBXO32-ΔF-box, exhibits the dominant negative form activity in mediating c-Myc degradation. The protein levels of c-Myc were further quantified (Fig. 1*D*). To further evaluate the data, we knocked down endogenous FBXO32 by transiently transfected pSuper-*FBXO32*-shRNA-1 and pSuper-*FBXO32*-shRNA-1 in HCT116 cells and examined the protein level at different time points in the presence of CHX (50 μg/ml). *Versus* the control, which was transiently transfected with pSuper-GFP-shRNA (*left panel* in Fig. 1*E*), knockdown of FBXO32 prolonged the half-life of endogenous c-Myc (*middle* and *right panels* in Fig. 1*E*). This is in contrast to what was seen in overexpression of FBXO32 (Fig. 1*E*). The c-Myc levels were then further quantified (Fig. 1*E*).

It is of note that anti-c-Myc antibodies from different companies could detect different expression patterns of endogenous c-Myc. The anti-c-Myc antibody from ABclonal could only detect one obvious band of endogenous c-Myc, but the antibody from Cell Signaling could detect two bands of endogenous c-Myc. Regardless of the number of bands, the tendency of c-Myc expression to be affected by knockdown of FBXO32 remained consistent (Fig. 1, *B*, *C*, and *E*). Taken together, these observations suggest that FBXO32 induces c-Myc degradation and that the F-box domain is required for FBXO32 to mediate c-Myc degradation.

Phosphorylation of c-Myc at Thr-58 and Ser-62 Is Dispensable for FBXO32-induced c-Myc Degradation—It has been reported that FBW7, an F-box E3 ligase, destabilizes c-Myc, but the FBW7 mutant lacking the F-box domain delayed it (15, 16), which is similar to what was observed for FBXO32. Of note, the turnover of c-Myc by FBW7 is largely dependent on the phosphorylation of Thr-58 and Ser-62 in MBI (15, 16). In addition, a common c-Myc mutant, P57S, in Burkitt lymphoma is able to abrogate Thr-58 phosphorylation (32). To determine whether FBXO32 also has functions similar to that of FBW7 on these

[2] The abbreviations used are: CHX, cycloheximide; K8R, K51R/K52R/K126R/K157R/K289R/K371R/K389R/K412R multiple mutant.

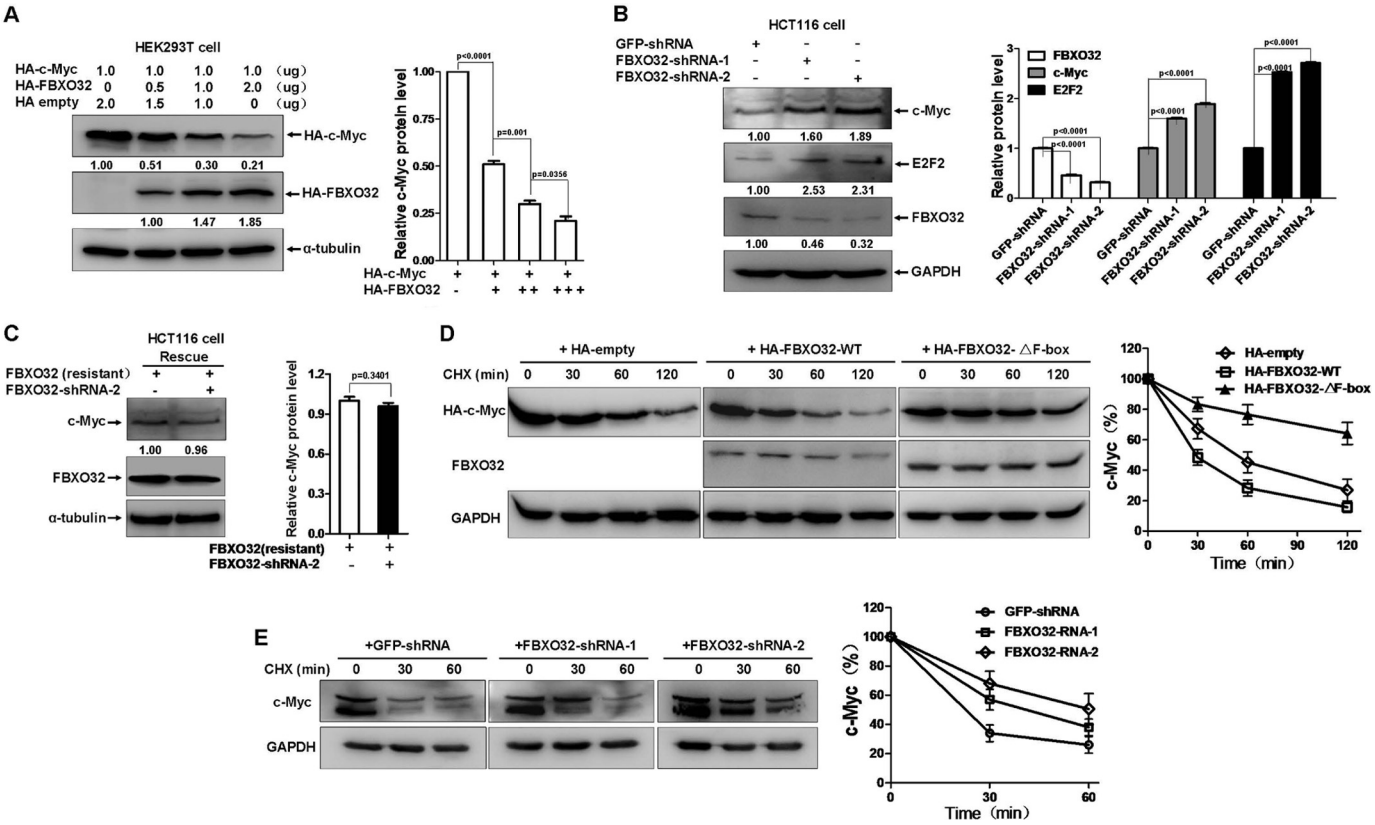

FIGURE 1. **FBXO32 promotes c-Myc turnover.** *A*, ectopic expression of HA-FBXO32 induced degradation of ectopic expressed HA-c-Myc. HEK293T cells were transfected with equal amounts of HA-c-Myc along with increasing amounts of HA-FBXO32, compensated with a CMV-HA empty vector to keep the same amount of transfected plasmid DNA. Quantization of the protein levels is shown on the *right*. *B*, knockdown of FBXO32 by shRNAs causes the protein levels of endogenous c-Myc and its target E2F2 to be increased in HCT116 cells. Quantification of the protein levels is shown on the *right*. *C*, ectopic expression of FBXO32-shRNA-2-resistant FBXO32 cDNA can rescue the effect of FBXO32-shRNA-2 on the endogenous protein level of c-Myc in HCT116 cells. Quantization of the protein levels is shown on the *right*. *D*, co-transfection of HA-FBXO32 enhances c-Myc protein instability in the presence of protein synthesis inhibitor CHX (50 μg/ml), but co-transfection of HA-FBXO32-ΔF-box (F-box deleted) does not. HCT116 cells were transiently transfected with the indicated plasmids. After 24 h, CHX was added to the cells, and cell lysates were prepared at the indicated time points. Quantization of the protein levels is shown on the *right*. *E*, knockdown of FBXO32 by FBXO32-shRNA-1 or FBXO32-shRNA-1 in HCT116 cells enhances endogenous c-Myc protein stability in the presence of protein synthesis inhibitor CHX (50 μg/ml). Quantization of the protein levels is shown on the *right*. Multi Gauge version 3.0 was used for quantifying protein levels based on band density obtained in Western blot assays; the statistical analysis was performed using GraphPad Prism version 5.0 (unpaired Student's *t* tests). *Error bars*, S.E.

mutants, we examined the effect of FBXO32 on the c-Myc mutants T58A, S62A, T58A/S62A, and P57S as well as the constitutive phosphorylation mutant S62E. As shown in Fig. 2, *A* and *B*, co-expression of HA-FBXO32 promotes degradation in all of these mutants. In addition to these three sites, four other sites (Ser-71, Tyr-74, Thr-358, and Ser-373) in c-Myc have also been reported to be phosphorylation sites (33–36). We found that HA-FBXO32 also promotes degradation in all four mutants (S71A, Y74A, T358A, and S373A) (Fig. 2*C*). These observations suggest that the turnover of c-Myc by FBXO32 is neither dependent on phosphorylation of Thr-58 and Ser-62 in MB1 nor dependent on phosphorylation of other sites, which is in contrast to FBW7 (15, 16).

FBXO32 Interacts with c-Myc—To determine the mechanisms of FBXO32-mediated c-Myc degradation, we examined whether FBXO32 could interact with c-Myc. As shown in Fig. 3*C*, ectopically expressed HA-c-Myc could pull down ectopically expressed FLAG-FBXO32 in HEK293T cells by immunoprecipitation assays using anti-HA-conjugated agarose beads (Fig. 3*A*). This interaction was endogenous and direct because a polyclonal anti-c-Myc antibody (A0309, ABclonal) pulled down endogenous FBXO32 in mouse muscle lysates (Fig. 3*B*), and GST-FBXO32 expressed in *Escherichia coli* pulled down His-c-Myc in *E. coli* (Fig. 3*C*). In addition, the c-Myc mutants T58A, S62A, and T58A/S62A could interact with FBXO32 when they were overexpressed in HEK293T cells (Fig. 3*D*).

We performed domain mapping to further study the mechanism of FBXO32-mediated c-Myc degradation. Whereas FLAG-tagged FBXO32 could be effectively pulled down by the truncated c-Myc mutants, 1–144 and 1–367 (Fig. 3, *E* and *F*), the other two truncated c-Myc mutants (168–367 and 168–439) only weakly pulled down FLAG-tagged FBXO32 (Fig. 3, *E* and *F*). The c-Myc truncated mutant (mutant 1–144) contains two conserved domains, MBI and MBII (Fig. 3*E*) (37). As reported, MBI is required for FBW7 interactions (15), whereas MBII is required for Skp2 interactions (18). To determine whether MBI or MBII is required for FBXO32 interaction, we performed fine domain mapping. Deletion of MBI or MBII did not impact the interaction between FBXO32 and the c-Myc mutant (mutant 1–144; Fig. 3*G*). We also examined whether the interaction between FBXO32 and the c-Myc mutant (mutant 168–367) requires the domain MBIII or MBIV or the

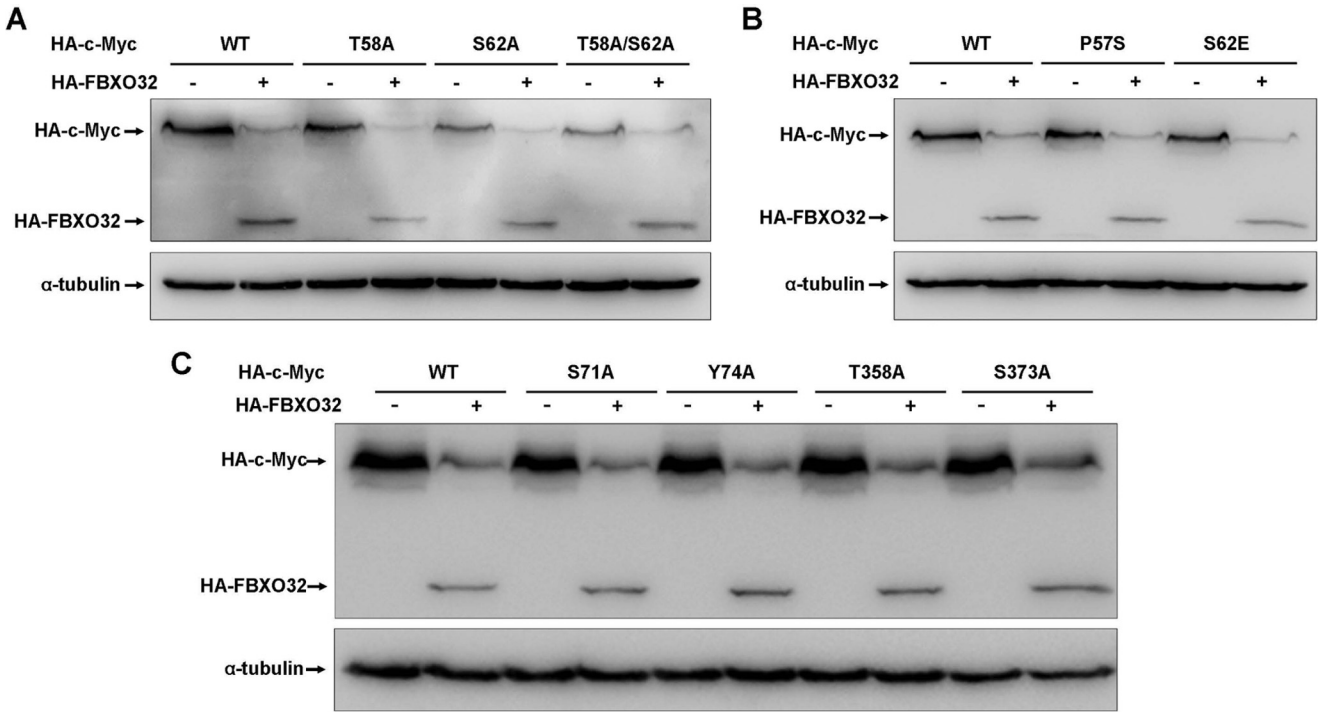

FIGURE 2. **FBXO32-mediated c-Myc degradation is independent of the phosphorylation of c-Myc at Thr-58 and Ser-62.** *A*, co-transfection of HA-FBXO32 causes protein degradation of wild-type c-Myc as well as c-Myc mutants T58A, S62S, and T58A/S62A. *B*, co-transfection of HA-FBXO32 causes protein degradation of wild-type c-Myc as well as c-Myc mutants P57S and S62E. *C*, co-transfection of HA-FBXO32 causes protein degradation of wild-type c-Myc as well as c-Myc mutants S71A, Y74A, T358A, and S373A.

PEST domains. Although the interaction between FBXO32 and the c-Myc mutant (mutant 168–367) was relatively weak, deletion of MBIII did not obviously impact the interaction between FBXO32 and the c-Myc mutant (mutant 168–367). Deletion of MBIV and PEST abrogated the interaction between FBXO32 and the c-Myc mutant (mutant 168–367), which suggests that the FBXO32 interacts with domain 168–367 of c-Myc and requires the MBIV and PEST.

We next sought to determine the FBXO32 domains required for c-Myc interaction. It appeared that all of the domains in the FBXO32 could pull down c-Myc, whereas the amino terminus (residues 1–223) or the carboxyl terminus alone interacted with c-Myc much more strongly. Of note, the truncated mutant of FBXO32 lacking the F-box domain (1–355(ΔF-box)) still interacted with c-Myc. To further determine whether the F-box domain is required for c-Myc interactions, we fused GFP to 218–355 and 271–355, respectively, and performed immunoprecipitation assays. As shown in Fig. 3*J*, c-Myc could interact with the domain 272–355 of FBXO32 as well as the domain 218–355 of FBXO32. This suggests that the F-box is definitely not required for FBXO32 to interact with c-Myc. In sum, the data suggest that FBXO32 interacts with c-Myc endogenously and directly.

FBXO32 Catalyzes c-Myc to Form Lys-48-linked Polyubiquitin Chain and Induces c-Myc for Proteasomal Degradation—To determine whether FBXO32 acts as an E3 ubiquitin ligase to induce c-Myc proteasomal degradation, we examined whether the potent proteasomal inhibitor, MG132, could block FBXO32-induced c-Myc degradation. We transfected HA-c-Myc into HEK293T cells as well as an HA empty vector control or HA-FBXO32. We then treated the cells with MG132 or DMSO (control) for 6 h before the harvest. The addition of MG132 effectively blocked FBXO32-induced c-Myc degradation (Fig. 4*A*), which indicates that FBXO32 mediates c-Myc proteasomal degradation.

We performed ubiquitination assays to confirm that FBXO32 can indeed catalyze c-Myc to form polyubiquitin chains (Fig. 4*B*). However, polyubiquitination of c-Myc reduced dramatically when the wild-type FBXO32 was replaced by the FBXO32 mutant that lacked the F-box domain. This suggested that FBXO32 requires the F-box domain to perform its E3 ubiquitin ligase role.

Ubiquitin contains seven lysine residues (Lys-6, -11, -27, -29, -33, -48, and -63) that can participate in either polyubiquitination or monoubiquitination to generate polyubiquitin or monoubiquitin involved in various biological functions (39). Lys-48-linked polyubiquitination is thought to target substrates for proteasomal degradation, whereas Lys-63-linked polyubiquitination has been implicated in multiple functions (40). We performed further assays to determine whether FBXO32 catalyzes c-Myc to form Lys-48-linked polyubiquitination. When the Lys-48 of ubiquitin was mutated to arginine, polyubiquitination of c-Myc by FBXO32 was reduced dramatically *versus* wild-type ubiquitin (Fig. 4*C*). However, when the Lys-63 of ubiquitin was mutated to arginine, polyubiquitination of c-Myc by FBXO32 was similar to that of wild-type ubiquitin (Fig. 4*C*). We next used seven Lys-only mutants of ubiquitin (Lys-6, -11, -27, -29, -33, -48, and -63) to perform polyubiquitination assays. These mutants only keep one lysine, and all of the other lysines are mutated to arginine (30). FBXO32 catalyzed c-Myc polyubiquitination in the presence of wild type (WT), Lys-48-only mutant, and Lys-11-only mutant but not other

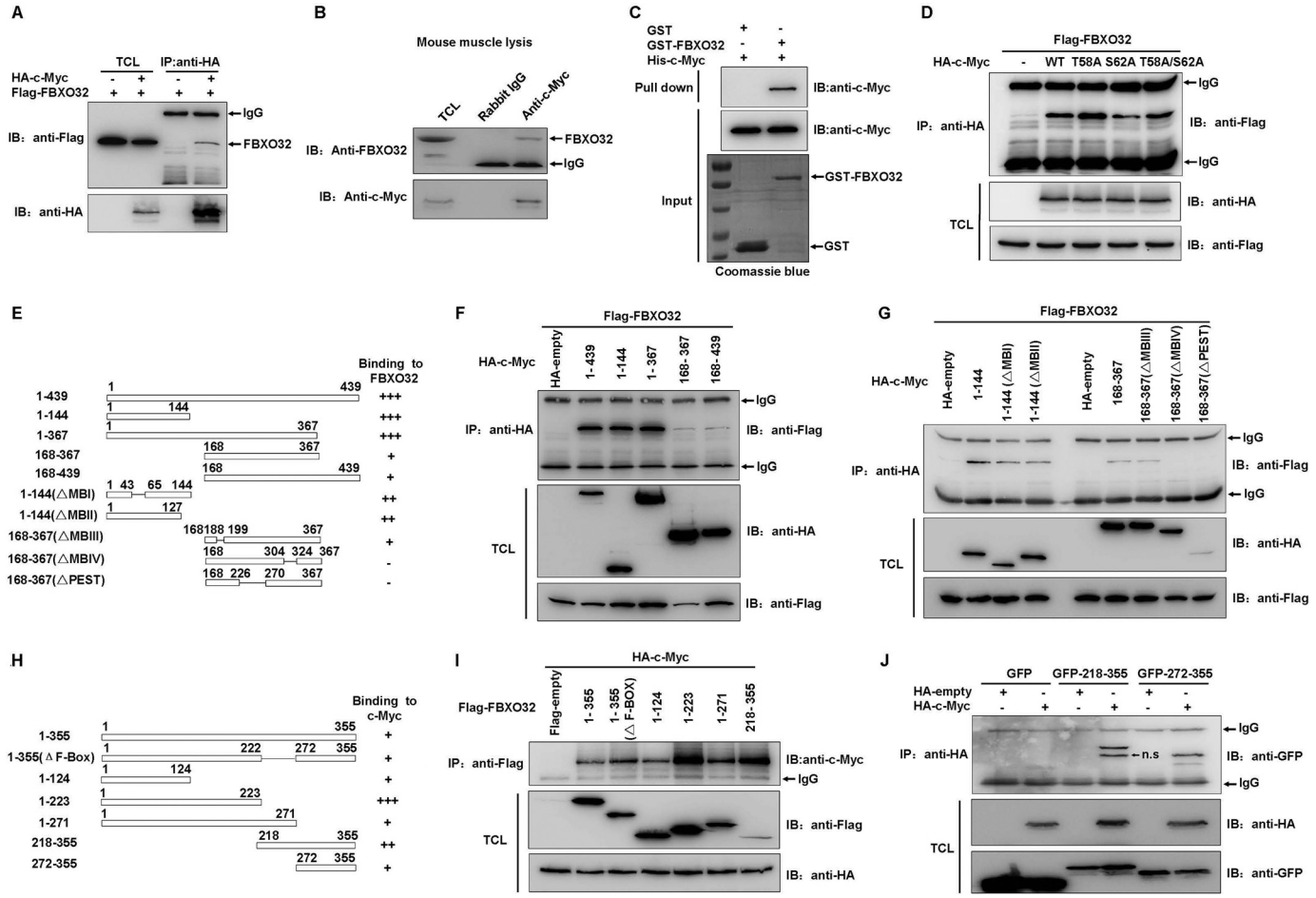

FIGURE 3. **FBXO32 directly interacts with c-Myc.** *A*, co-immunoprecipitation assays show FLAG-tagged FBXO32 interacts with HA-tagged c-Myc when they are overexpressed in HEK293T cells. *B*, endogenous FBXO32 interacts with endogenous c-Myc, as revealed by co-immunoprecipitation assays using anti-c-Myc antibody in mouse muscle lysates. Rabbit IgG is used as control for co-immunoprecipitation assays. *C*, bacterial expressed GST-tagged FBXO32 directly interacts with bacterial expressed His-tagged c-Myc. Bacterial expressed GST protein is used as control. *D*, the wild-type c-Myc as well as its mutants T58A, S62A, and T58A/S62A interact with FBXO32, as revealed by co-immunoprecipitation assays. *E*, schematic of the c-Myc domains. The extent of the interaction between FBXO32 and the c-Myc domains is indicated by the number of *plus signs*. *F* and *G*, co-immunoprecipitation of human FLAG-FBXO32 with HA-tagged c-Myc domains in HEK293T cells transfected with the indicated plasmids. *H*, schematic of the FBXO32 domains. The extent of the interaction between c-Myc and the FBXO32 domains is indicated by the number of *plus signs*. *I*, co-immunoprecipitation of human HA-c-Myc with FLAG-tagged FBXO32 domains in HEK293T cells transfected with the indicated plasmids. *J*, co-immunoprecipitation of human HA-c-Myc with GFP-tagged FBXO32 domains in HEK293T cells transfected with the indicated plasmids. *IP*, immunoprecipitation; *IB*, immunoblot; *n.s.*, nonspecific; *TCL*, total cell lysate.

Lys-only mutants (Fig. 4*D*). These phenomena indicate that FBXO32 could indeed catalyze c-Myc to form Lys-48-linked polyubiquitin chains, which is consistent with its role in mediating c-Myc for proteasomal degradation.

FBXO32 Targets c-Myc Ubiquitination at Lys-326—To identify the lysine residue(s) in c-Myc catalyzed by FBXO32, we systematically mutated them to arginine. The protein degradation efficiency by FBXO32 was used to monitor the potential ubiquitination site(s) in c-Myc. Fig. 5*A* illustrates that overexpression of FBXO32 did not promote degradation of one mutant (K326R). Although the mutant (K326R) showed the most dramatic increase of resistance to FBXO32-mediated degradation, it looks like additional sites (K51R/K52R, K126R, K157R, K289R, K371R, K389R, and K412R) also exhibited some resistance. To further confirm that Lys-326 is the key site catalyzed by FBXO32, we made additional mutants K51R, K52R, K51R/K52R/K126R/K157R/K289R/K371R/K389R/K412R (K8R), and K326R+K8R and repeated the experiments. The mutants K51R, K52R, and K8R could still be degraded by FBXO32, although K8R exhibited some resistance (Fig. 5, *B* and *C*). When Lys-326 was mutated in K8R (K326R+K8R), the mutant showed complete resistance (Fig. 5*C*). The quantitative data are summed in Fig. 5*D*. *Versus* the wild-type c-Myc, polyubiquitination of the c-Myc(K326R) mutant by the wild-type FBXO32 was clearly decreased, but it did not completely disappear (Fig. 5*E*). It appears that this reduction was not a result of the reduction of interaction between FBXO32 and c-Myc(K326R) because c-Myc(K326R) could still interact with c-Myc as well as the wild-type c-Myc (Fig. 5*F*). Interestingly, *versus* the wild-type c-Myc, polyubiquitination of the c-Myc K8R mutant by the FBXO32 was also decreased, and polyubiquitination of the c-Myc K326R+K8R mutant induced by FBXO32 completely disappeared.

FBXO32 Suppresses c-Myc Activity—To evaluate the biological consequences of FBXO32-mediated c-Myc degradation, we examined the effect of FBXO32 on the transactivation of two well defined c-Myc target genes, *Gadd45α* (42)and *E2F2* (43). As expected, ectopic expression of c-Myc inhibited the

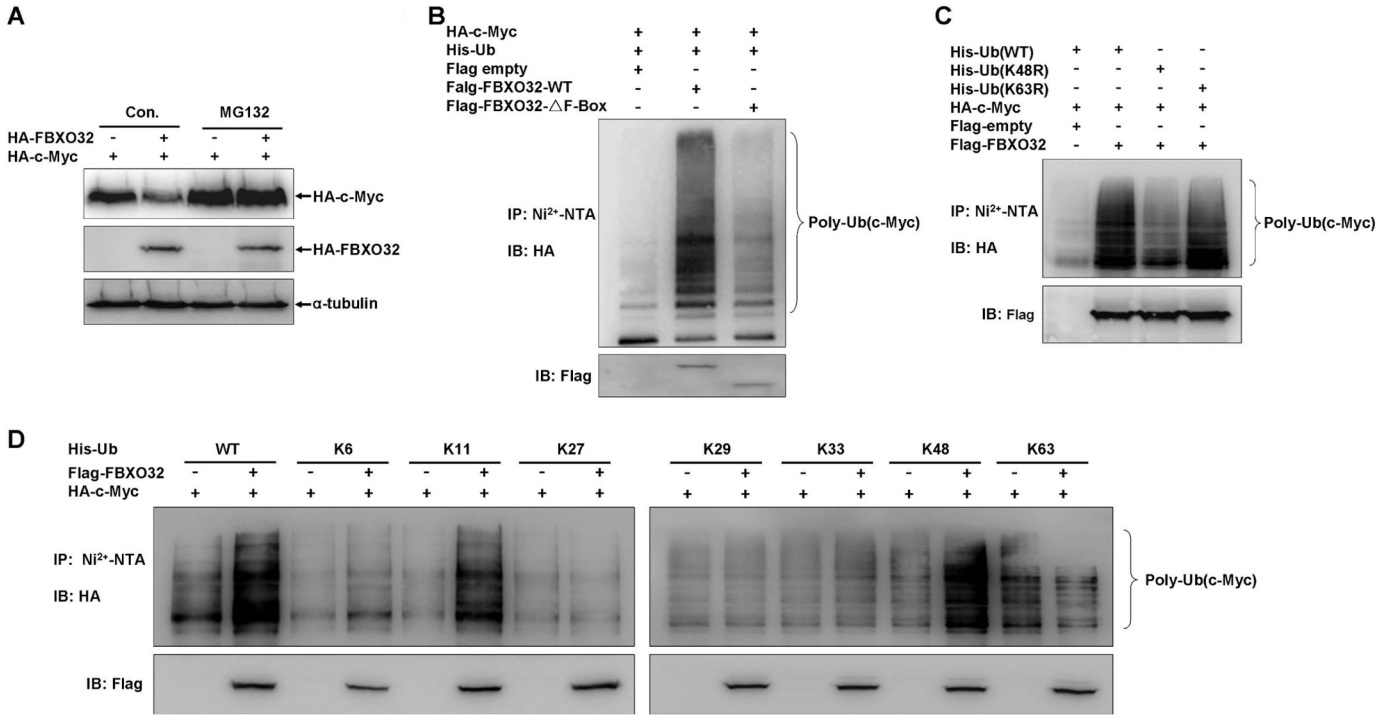

FIGURE 4. **FBXO32 catalyzes c-Myc for Lys-48-linked ubiquitination and proteasomal degradation.** *A*, the proteasome inhibitor MG132 blocks FBXO32-induced c-Myc degradation. HEK293T cells were transfected with HA-c-Myc together with either HA-FBXO32 or empty vector; MG132 (20 μM) was added to the medium 6 h before protein harvest. *B*, the wild-type FBXO32 (FLAG-FBXO32-WT) catalyzes c-Myc ubiquitination, but when the F-box is deleted, the mutant (FLAG-FBXO32-ΔF-Box) reduces its catalytic capability dramatically for c-Myc ubiquitination. HEK293T cells were transfected with HA-c-Myc and His-Ub-WT or alone with FLAG-FBXO32-WT or FLAG-FBXO32-ΔF-box; 24 h after transfection, lysates were prepared and subjected to immunoprecipitation by Ni^{2+}-nitrilotriacetic acid beads and then were detected by Western blot using anti-HA antibody. *C*, the wild-type FBXO32 (FLAG-FBXO32-WT) catalyzes c-Myc for Lys-48-linked ubiquitination but not for Lys-63-linked ubiquitination. HEK293T cells were transfected with HA-c-Myc and FLAG-FBXO32 or alone with His-tagged wild-type ubiquitin (*His-Ub-WT*), His-tagged ubiquitin 48 Lys/Arg mutant (*Ub-K48R*), or His-tagged ubiquitin 63 Lys/Arg mutant (*His-Ub-K63R*); the ubiquitination assays were performed as in *B*. *D*, Lys-48-linked ubiquitination catalyzed by the wild-type FBXO32 (FLAG-FBXO32-WT) was further confirmed by seven Lys-only ubiquitin mutants, Lys-6, -11, -27, -29, -33, -48, and -63. *IP*, immunoprecipitation; *IB*, immunoblot.

Gadd45α promoter activity ~0.23-fold ($p = 0.0050$) (Fig. 6*A*) in HEK293T cells. However, co-expression of FBXO32 together with c-Myc restored the suppressive role of c-Myc in *Gadd45α* promoter activity ($p = 0.0044$) (Fig. 6*A*). The c-Myc activated the *E2F2* promoter activity ~2.55-fold. Co-expression of FBXO32 together with c-Myc abrogated the *E2F2* promoter activity induced by c-Myc ($p = 0.0190$). In contrast, c-Myc had no activating role in the mutated *E2F2* promoter activity ($p = 0.1107$) (Fig. 6*C*). Co-expression of FBXO32 also could not exhibit its suppressive role in the mutated *E2F2* promoter activity (Fig. 6*C*). The expressions of ectopically expressed HA-c-Myc and HA-FBXO32 in HEK293T cells were confirmed by Western blot analysis (Fig. 6*D*).

To further evaluate the role of FBXO32 in c-Myc activity, we established stable A673 cell lines (a rhabomyosarcoma cell line) with overexpression of FBXO32 or knockdown of FBXO32 by transduced A673 cells using lentiviral infection. The endogenous FBXO32 protein levels in mouse muscle, A673 cells, and HCT116 cells were examined by Western blot assay (data not shown). Overexpression of FBXO32 reduced the *E2F2* mRNA level but caused an increase in the *Gadd45α* mRNA level, as revealed by semiquantitative RT-PCR analysis (Fig. 6, *E* and *F*). In contrast, knockdown of FBXO32 by either FBXO32-shRNA-1 or FBXO32-shRNA-2 caused an increase in the *E2F2* mRNA level, but this reduced the *Gadd45α* mRNA level, as revealed by semiquantitative RT-PCR analysis (Fig. 6, *G* and *H*). These observations are consistent with the data obtained from the promoter assays.

To determine whether FBXO32-mediated regulation of *Gadd45α* and *E2F2* is dependent on c-*Myc*, we generated three stable HCT116 cell lines with lentiviral infection. The first cell line expressed c-Myc-shRNA, which targets the 5′-UTR region of c-Myc. The second and third cell lines were established by reinfecting the first cell line with lentiviruses expressing the wild-type c-Myc and c-Myc(K326R) mutant, respectively. In cells with c-Myc-knocked down, overexpression of FBXO32 had no obvious effect on *Gadd45α* and *E2F2* promoter activity (Fig. 6, *I* and *M*). In contrast, the effects of FBXO32 on *Gadd45α* promoter activity and the inhibition of FBXO32 on *E2F2* promoter activity were recovered with c-Myc restoration (Fig. 6, *J* and *N*). However, in the third cell line with c-Myc(K326R) mutant expression, the activation of FBXO32 on *Gadd45α* promoter activity and the inhibition of FBXO32 on the *E2F2* promoter activity were not recovered (Fig. 6, *K* and *O*). The expressions of wild-type c-Myc, c-Myc(K326R), and HA-FBXO32 were confirmed by Western blot analysis (Fig. 6*L*). Whenever c-Myc was knocked down by c-Myc-shRNA or wild-type c-Myc was restored in c-Myc-knocked down cells, overexpression of FBXO32 had no effect on the E-box-mutated *E2F2* promoter activity (Fig. 6, *P* and *Q*). These observations suggest that FBXO32-mediated regulation of *Gadd45α* and *E2F2* is depen-

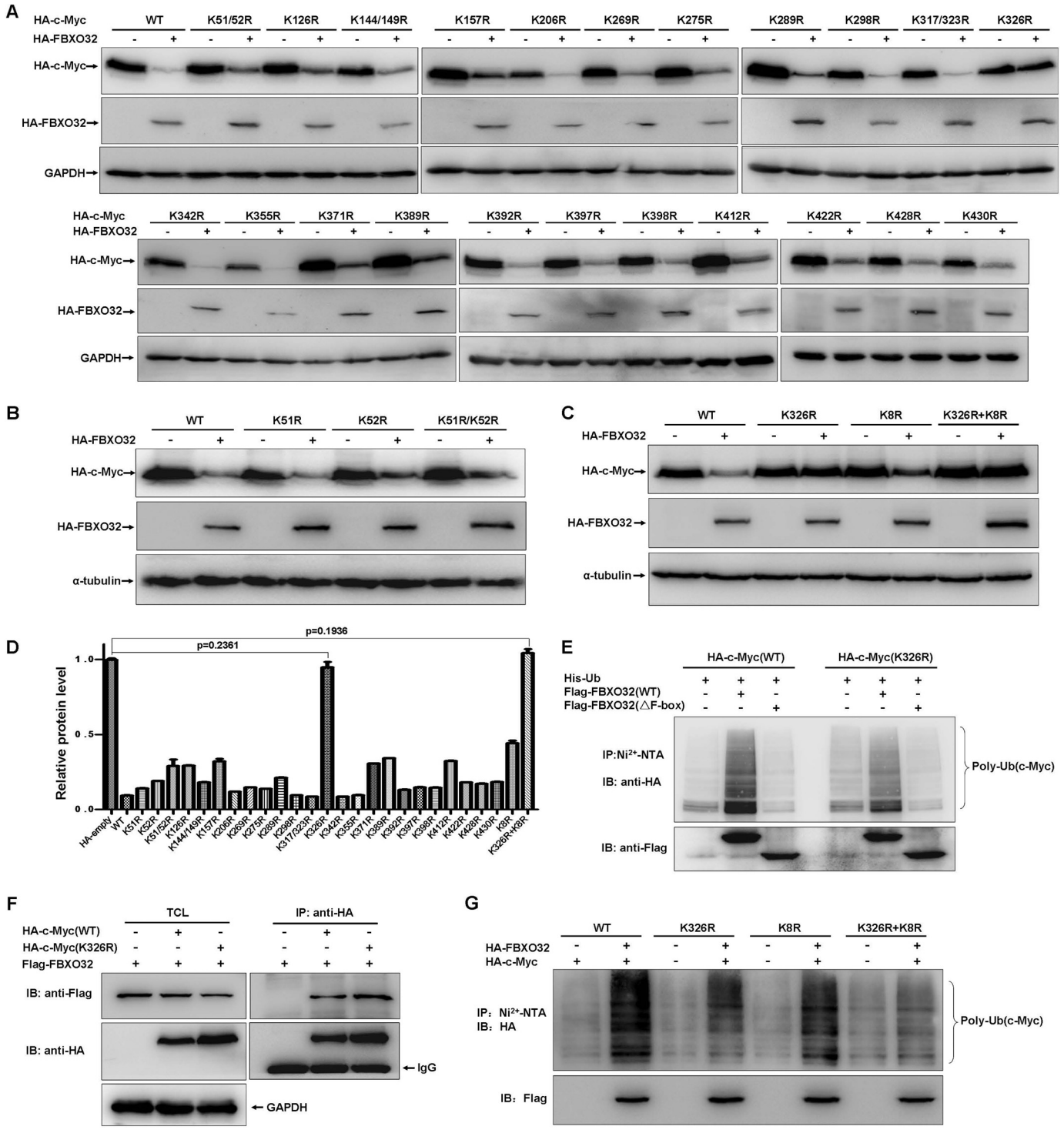

FIGURE 5. **FBXO32 targets c-Myc ubiquitination at K326.** *A*, HEK293T cells were transfected with the indicated c-Myc mutants together with either FBXO32 or empty vector. The expressions of c-Myc were detected by Western blot analysis using anti-HA antibody. *B*, degradation of the c-Myc mutants, K51R, K52R, and K51R/K52R induced by FBXO32 was further confirmed. *C*, degradation of the c-Myc multiple mutant, K8R, was further confirmed. *D*, protein levels were quantified based on band density obtained in Western blot assays; the protein level with HA empty vector transfection was treated as 1; the statistical analysis was performed using GraphPad Prism version 5.0 (unpaired Student's *t* tests); the protein level with HA empty vector transfection was treated as 1. *E*, the catalytic capability of FBXO32 on c-Myc(Lys-326) polyubiquitination is reduced significantly (the sixth column from the *left* to the *right*) compared with that on wild-type c-Myc (the *second column* from the *left* to the *right*). *F*, the c-Myc Lys/Arg mutant (HA-c-Myc(K326R)), as well as the wild-type c-Myc (HA-c-Myc(WT)), interacts with FBXO32, as revealed by co-immunoprecipitation assays. For ectopic expression, the amount of HA-c-Myc(WT) was 2 times more than that of HA-c-Myc(K326R) (ratio = 1:3) regarding the degradation of wild-type c-Myc by FBXO32. *G*, the catalytic capability of FBXO32 on the c-Myc multiple mutant (K326R plus K8R) polyubiquitination is further reduced (the *eighth column* from the *left* to the *right*) compared with that on the c-Myc(K326R) (the *fourth column* from the *left* to the *right*). *Error bars*, S.E. *IP*, immunoprecipitation; *IB*, immunoblot.

dent on c-*Myc*. Taken together, these data suggest that FBXO32 suppresses c-Myc activity.

FBXO32 Inhibits Ovary Cancer Cell SKOV3 Proliferation—To elucidate the biological function of FBXO32 in mediating c-Myc degradation, we examined its effect on cell proliferation using three stable SKOV3 cell lines generated by lentiviral infection, vector control, FBXO32, and FBXO32-ΔF-box. *Versus* the control cells, the SKOV3 cells with the FBXO32 overexpression proliferated much more slowly from day 2 (Fig. 7*A*). In contrast, the proliferation rate of the SKOV3 cells with stable FBXO32-ΔF-box mutant expression is similar to that of the control cells. Conversely, the SKOV3 cells with stable knocked down FBXO32 proliferated faster than the control cells expressing GFP shRNA (Fig. 7*B*).

Through the colony formation assays, we further found that the colony number formed in the SKOV3 cells with the FBXO32 overexpression was fewer than that of the control SKOV3 cells or that of the SKOV3 cells with the FBXO32-ΔF-box overexpression (Fig. 7*D*). Thus, FBXO32 can inhibit cell proliferation, which might be mediated by inducing c-Myc degradation.

FBXO32 Is a Direct Target Gene of c-Myc—As a transcription factor, c-Myc can form heterodimers with MAX that bind to E-boxes in the regulatory regions of the target genes and regulate a broad spectrum of genes involved in multiple physiological and pathological processes (44). After we performed bioinformatic analysis on the promoter region of *FBXO32*, we realized a potential E-box localized at the positions −107 to

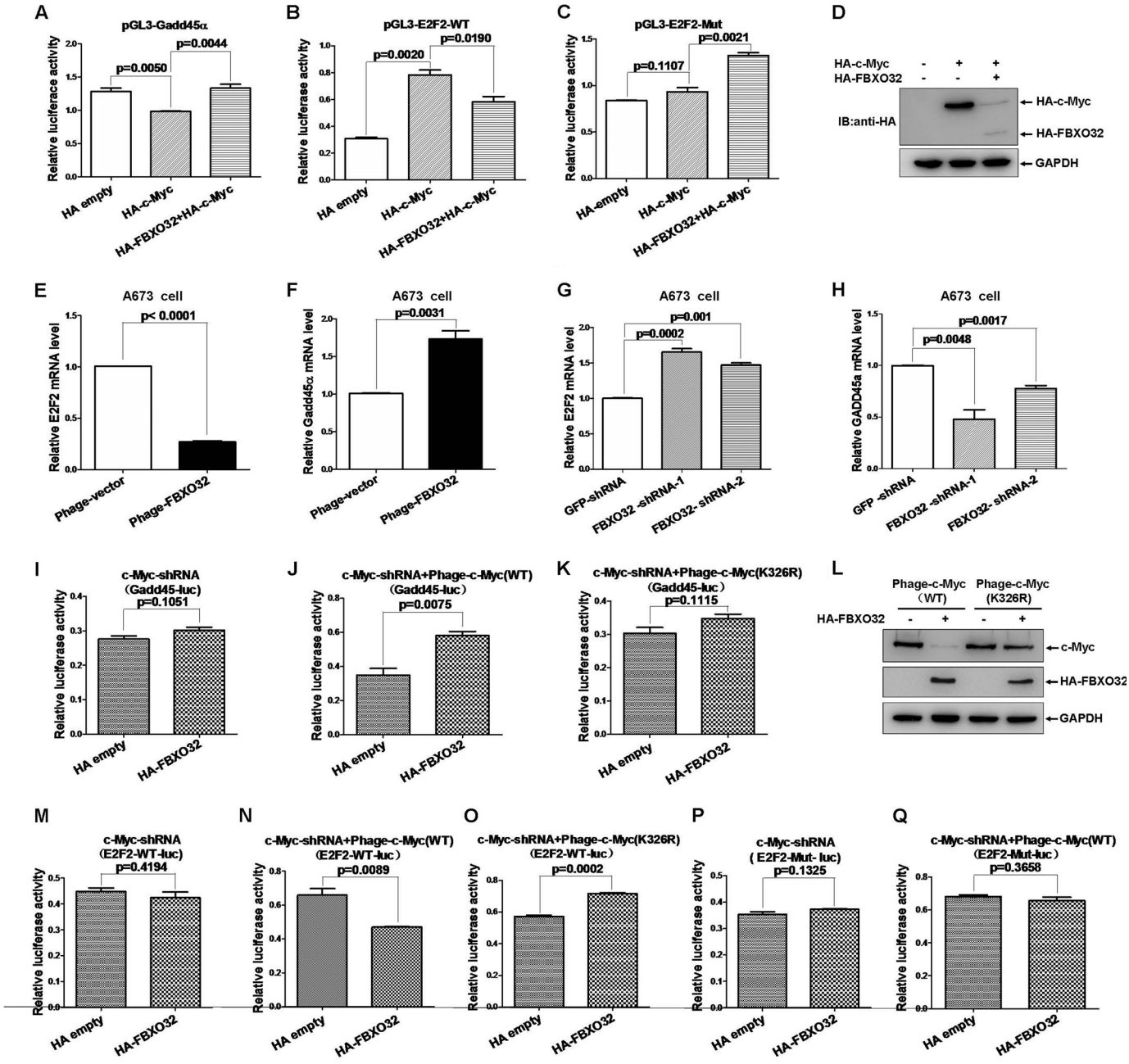

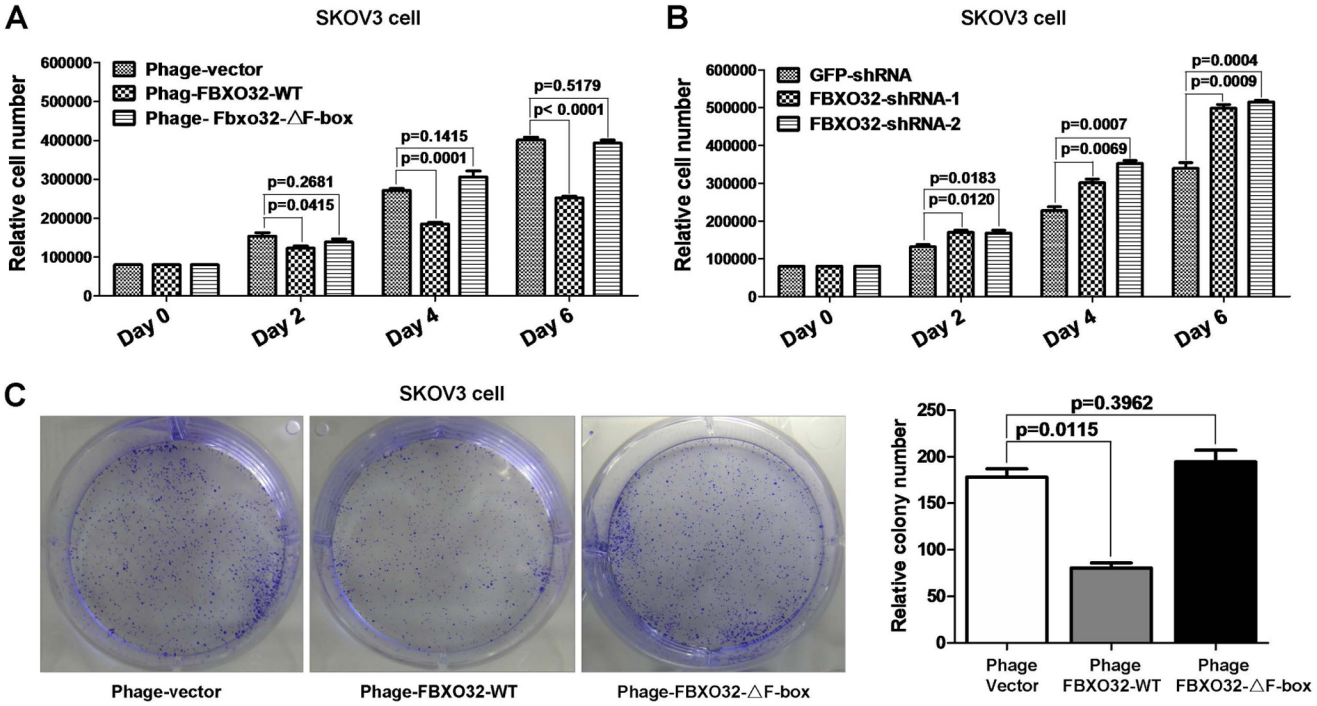

FIGURE 7. **FBXO32 inhibits ovary cancer cell SKOV3 proliferation.** *A*, overexpression of wild-type *FBXO32* by lentivirus infection in SKOV3 cells inhibits cell proliferation significantly after day 2 compared with the control, but overexpression of F-box-deleted mutant of FBXO32 (FBXO32-ΔF-box) has no obvious effect. The SKOV3 cells transduced with lentivirus vectors stably expressing GFP and *FBXO32* or GFP alone (as a control) were seeded in 6-well plates with 8×10^3 cells/well. *B*, knockdown of FBXO32 by *FBXO32*-shRNA-1 or *FBXO32*-shRNA-2 in SKOV3 cells enhances cell proliferation after day 2 compared with the control. The SKOV3 cells transduced with lentivirus vectors stably expressing *FBXO32*-shRNA-1, *FBXO32*-shRNA-2, or GFP-shRNA (as a control) were seeded in 6-well plates with 8×10^3 cells/well. The cell numbers were counted every 2 days using an automated cell counter (Bio-Rad, TC20™). *C*, overexpression of wild-type FBXO32 inhibits colony formation, but overexpression of F-box-deleted mutant of FBXO32 (FBXO32-ΔF-box) has no obvious effect. Data are presented as mean ± S.E. (*error bars*) of three independent experiments performed in triplicate; the statistical analysis was performed using GraphPad Prism version 5.0 (*t* tests).

−102 (the translation initial site is designated as +1). Therefore, we sought to determine whether *FBXO32* is a direct target of c-Myc. We first amplified the *FBXO32* promoter spanning −425 to +24 and −204 to −5 by PCR and cloned this into the pGL4.10 vector (Promega). The promoter assays showed that ectopic expression of c-Myc caused a significant increase in *FBXO32* promoter activity (Fig. 8*A*). The expression of HA-c-Myc was confirmed by Western blot analysis (Fig. 8*B*). However, when the core sequence of the E-box (CACGTG) in the −204 to −5 region of the *FBXO32* promoter was mutated (CAGCTG), ectopic expression of c-Myc had no obvious effect on the activation of the mutated *FBXO32* promoter activity *versus* that of wild-type *FBXO32* promoter activity (Fig. 8, *C* and *D*). Moreover, overexpression of c-Myc in HEK293T cells and HCT116 cells caused an increase in *FBXO32* mRNA level (Fig. 8, *E* and *F*). Consistently, knockdown of c-Myc in HCT116 cells by c-Myc-shRNA-1 and c-Myc-shRNA-2 reduced the *FBXO32* mRNA level. The induction of FBXO32 by c-Myc

FIGURE 6. **FBXO32 inhibits c-Myc transcriptional activity.** *A*, overexpression of FBXO32 enhances the activity of *Gadd45α* promoter reporter activity suppressed by c-Myc ($p = 0.0044$) in HEK293T cells. *B* and *C*, overexpression of FBXO32 suppresses the activity of *E2F2* wild-type promoter reporter activity induced by c-Myc ($p = 0.0190$) but not the activity of *E2F2* promoter mutated reporter in HEK293T cells. *D*, the expressions of transfected HA-FBXO32 and HA-c-Myc in HEK293T cells are confirmed by Western blot using anti-HA antibody. *E*, the mRNA level of *E2F2* is reduced dramatically when FBXO32 is overexpressed by the lentivirus infection expressing FBXO32 (Phage-FBXO32) compared with the control with the lentivirus infection expressing GFP protein in A673 cells. *F*, the mRNA level of *Gadd45α* is increased dramatically when FBXO32 is overexpressed by the lentivirus infection expressing FBXO32 (Phage-FBXO32) compared with the control with the lentivirus infection expressing GFP protein in A673 cells. *G*, the mRNA level of *E2F2* is increased dramatically when FBXO32 is knocked down by the lentivirus infection expressing FBXO32-shRNA-1 and FBXO32-shRNA-2 compared with the control with the lentivirus infection expressing GFP-shRNA in A673 cells. *H*, the mRNA level of *Gadd45α* is reduced dramatically when FBXO32 is knocked down by the lentivirus infection expressing FBXO32-shRNA-1 and FBXO32-shRNA-2 compared with the control with the lentivirus infection expressing GFP-shRNA in A673 cells. *I*, overexpression of FBXO32 by lentivirus infection has no effect on *Gadd45α* promoter reporter activity in c-Myc-knocked down HCT116 cells ($p = 0.1051$). *J*, when c-Myc(WT) is re-expressed in c-Myc-knocked down HCT116 cells by lentivirus infection, the enhancement effect of FBXO32 on the activity of *Gadd45α* promoter reporter activity suppressed by c-Myc is restored ($p = 0.0075$). *K*, when the mutated c-Myc(K326R) is re-expressed in c-Myc-knocked down HCT116 cells by lentivirus infection, the enhancement effect of FBXO32 on the activity of *Gadd45α* promoter reporter activity suppressed by c-Myc is still not restored ($p = 0.1115$). *L*, the expressions of the HA-tagged wild-type c-Myc, the HA-tagged mutated c-Myc(K326R), and the HA-tagged FBXO32 by lentivirus infection in HCT116 cells are confirmed by Western blot analysis. *M*, overexpression of FBXO32 by transient transfection has no effect on *E2F2* promoter reporter activity in c-Myc-knocked down HCT116 cells ($p = 0.4194$). *N*, when c-Myc(WT) is re-expressed in c-Myc-knocked down HCT116 cells by lentivirus infection, the inhibitory effect of FBXO32 on the activity of *Gadd45α* promoter reporter activity up-regulated by c-Myc is restored ($p = 0.0002$). ○, when the mutated c-Myc(K326R) is re-expressed in c-Myc-knocked down HCT116 cells by lentivirus infection, the inhibitory effect of FBXO32 on the activity of *Gadd45α* promoter reporter activity up-regulated by c-Myc is still not restored ($p = 0.1325$). *P*, overexpression of FBXO32 by transient transfection has no effect on mutated *E2F2* promoter reporter (*E2F*-mut-luc) activity in c-Myc-knocked down HCT116 cells ($p = 0.1325$). *Q*, when the wild-type c-Myc(WT) is re-expressed in c-Myc-knocked down HCT116 cells by lentivirus infection, the inhibitory effect of FBXO32 on the activity of mutated *E2F2* promoter reporter activity up-regulated by c-Myc is still restored ($p = 0.3658$). Data are presented as mean ± S.E. (*error bars*) of three independent experiments performed in triplicate; the statistical analysis was performed using GraphPad Prism version 5.0 (unpaired Student's *t* tests). *IB*, immunoblot.

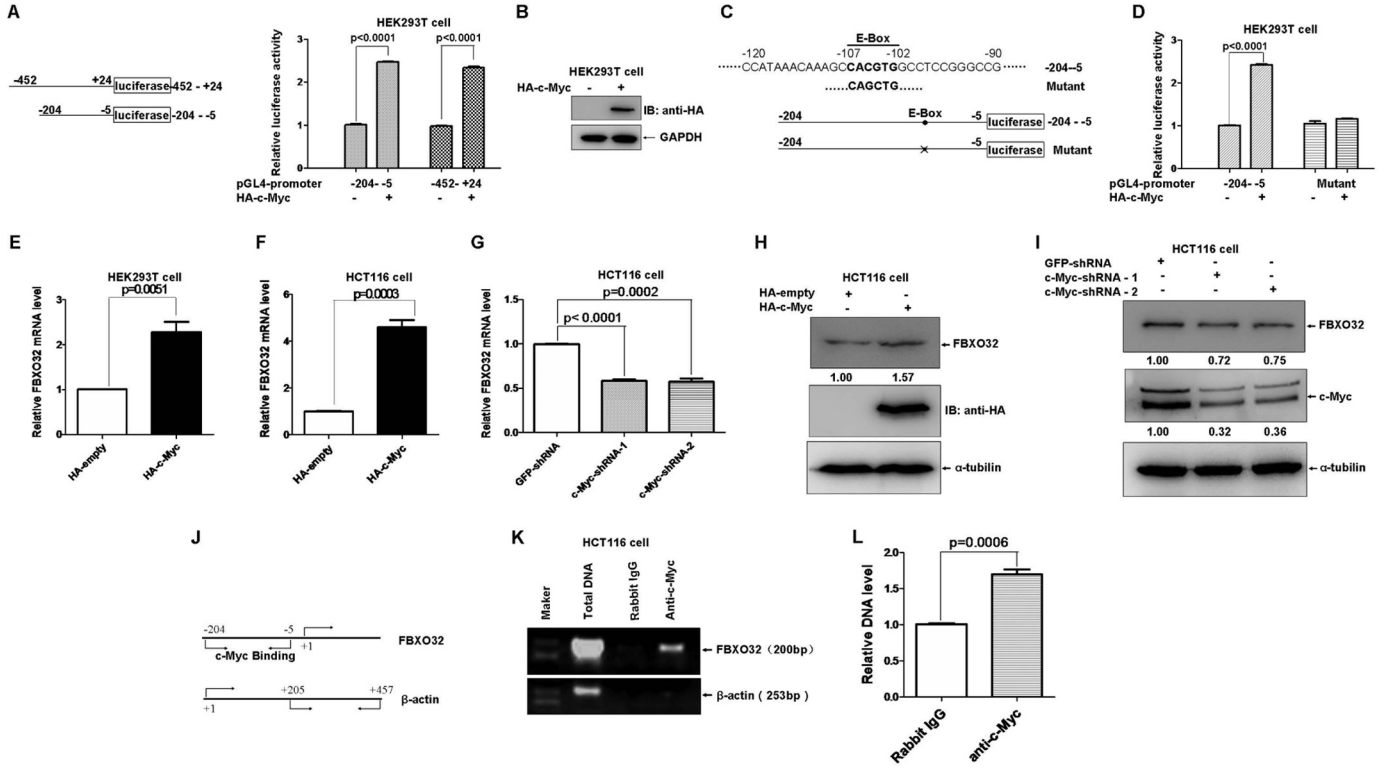

FIGURE 8. ***FBXO32* is a direct target of c-Myc.** *A*, overexpression of c-Myc activates *FBXO32* promoter reporter activity. A schematic of the *FBXO32* promoter reporter constructs is shown on the *left*. *B*, the expression of HA-c-Myc is confirmed by Western blot analysis. *C*, schematic of one potential c-Myc binding site (E-box: CACGTG (in *boldface type*)) localized at the *FBXO32* promoter (−204 to −5) and the mutated E-box construct. *D*, overexpression of c-Myc activates the wild-type *FBXO32* promoter reporter (−204 to −5) activity but not the mutated *FBXO32* promoter reporter activity. *E*, the mRNA level of *FBXO32* is elevated when c-Myc is overexpressed in HEK293T cells, as revealed by a semiquantitative RT-PCR assay ($p = 0.0061$). *F*, the mRNA level of *FBXO32* is elevated when c-Myc is overexpressed in HCT116 cells, as revealed by semiquantitative RT-PCR assays ($p = 0.0003$). *G*, the mRNA level of *FBXO32* is reduced when c-Myc is knocked down in HCT116 cells by c-Myc-shRNA-1 and c-Myc-shRNA-2, as revealed by semiquantitative RT-PCR assays. *H*, the protein level of *FBXO32* is elevated when c-Myc is overexpressed in HCT116 cells, as revealed by Western blot analysis using anti-c-Myc antibody. *I*, the protein level of *FBXO32* is reduced when c-Myc is knocked down in HCT116 cells by c-Myc-shRNA-1 and c-Myc-shRNA-2 as revealed by Western blot analysis. *J*, schematic of locations of fragments amplified in *FBXO32* promoter or β-actin promoter. *K*, ChIP analysis indicates that c-Myc interacts directly with the *FBXO32* promoter region harboring the E-box. *L*, semiquantitative RT-PCR analysis confirms that c-Myc binds to the −204 to −5 region of the *FBXO32* promoter. Data are presented as the means ± S.E. (*error bars*) of three independent experiments performed in triplicate.

was further confirmed by Western blot analysis in the status with either overexpression of c-Myc or knockdown of c-Myc (Fig. 8, *H* and *I*).

To determine whether c-Myc can directly bind to the promoter of *FBXO32*, we performed ChIP analysis. Fig. 8, *J* and *K*, illustrates that the anti-c-Myc antibody could pull down a 200-bp fragment containing the E-box that is located in the −204 to −5 region of the FBXO32 promoter *versus* the rabbit IgG control. Semiquantitative RT-PCR further confirmed co-precipitation of the anti-c-Myc with the promoter of *FBXO32* (Fig. 8*L*).

Considered collectively, these data suggest that c-Myc could up-regulate FBXO32 expression by directly binding to the *FBXO32* promoter. Thus, *FBXO32* might be a direct target of c-Myc.

Discussion

FBXO32 Targets c-Myc for Proteasomal Degradation—FBXO32 was identified as a muscle-specific E3 ubiquitin ligase more than 10 years ago. Increasing evidence indicates that *FBXO32* plays important roles in skeletal muscle atrophy as well as in tumorigenesis. In this study, we identified c-Myc as a novel target of FBXO32 for proteasomal degradation. First, we showed that FBXO32 promoted c-Myc degradation efficiently, which was effectively blocked by MG132. This suggested that FBXO32 serves as an E3 ubiquitin ligase to mediate c-Myc proteasomal degradation. Similar to the eIF3-f and MyoD degradation targets, the F-box domain is required for FBXO32 to induce c-Myc ubiquitination and degradation, resembling the F-box-containing E3 ubiquitin ligase (6, 7, 45).

Through mutant screening, we identified that Lys-326 of c-Myc might be the key position needed for FBXO32 to catalyze the formation of Lys-48-linked polyubiquitin chain because FBXO32 could not induce c-Myc(K326R) mutant degradation. Although the capability of the polyubiquitin chain formation catalyzed by wild-type FBXO32 was clearly reduced, the FBXO32 still could stimulate formation of polyubiquitin chains on c-Myc(K326R) mutants. This phenomenon suggests that FBXO32 might also catalyze formation of other kinds of polyubiquitin chains (except Lys-48 polyubiquitin chains) or catalyze other lysine sites (except Lys-326) to form polyubiquitin chains. Interestingly, we noticed that the c-Myc mutant K326R+K8R completely lost the ability to

form a polyubiquitin chain, and FBXO32 could also catalyze c-Myc to form Lys-11-only polyubiquitin chains. This may support the hypothesis.

The effect of FBXO32 on c-Myc is quite similar to that of FBW7, which is another well defined F-box E3 ubiquitin ligase that targets c-Myc for proteasomal degradation and inhibits c-Myc activity. However, phosphorylation of Thr-58 and Ser-62 is required for c-Myc degradation mediated by FBW7. In contrast, phosphorylation of Thr-58 and Ser-62 is not required for c-Myc degradation mediated by FBXO32, which suggests that FBXO32 mediates c-Myc degradation through a mechanism different from that of FBW7.

FBXO32 May Perform Its Tumor-suppressive Function through Targeting c-Myc—To date, the role of *FBXO32* in tumorigenesis remains debatable. Whereas FBXO32 is considered a hallmark of cancer cachexia (13, 46), FBXO32 is also found to be down-regulated in some types of cancer through different mechanisms (9, 47), suggesting its tumor-suppressive function. In this study, we showed that FBXO32 could effectively induce degradation of c-Myc, a classic oncogene overactivated in many types of cancer (48). Moreover, we found that overexpression of FBXO32 suppresses growth of ovary cancer SKOV3 cells but that knockdown of FBXO32 enhances growth of SKOV3 cells. These findings reinforce the tumor-suppressive function of FBXO32. As a muscle-specific gene, further exploring the role of FBXO32 in the initiation and progression of some special types of cancer that developed from muscle tissues (*i.e.* rhabdomyosarcoma) will shed light on the role of FBXO32 in tumorigenesis.

Negative Feedback Regulation of c-Myc by FBXO32—In this study, we also identified *FBXO32* as a direct downstream target of c-*Myc*, revealing a negative feedback regulation loop between c-Myc and FBXO32. c-Myc transcriptionally regulates FBXO32 expression, but FBXO32 promotes c-Myc degradation. Actually, another E3 ubiquitin ligase of c-Myc (17, 18), Skp2, is also up-regulated by c-Myc, although it serves as a co-factor instead of a suppressor for c-Myc-regulated transcription (41). Notably, this type of regulation has been widely recognized, including the p53/MDM2 (38) pathway, which implicates a strict regulation mechanism between the two genes. Further understanding of this regulation loop will open a new window for understanding the mechanisms of these two genes in tumorigenesis.

Acknowledgments—We are grateful to Drs. Stephen Hann, Scott Lowe, and Linda Penn for the generous gifts of reagents.

References

1. Bodine, S. C., Latres, E., Baumhueter, S., Lai, V. K. M., Nunez, L., Clarke, B. A., Poueymirou, W. T., Panaro, F. J., Na, E. Q., Dharmarajan, K., Pan, Z. Q., Valenzuela, D. M., DeChiara, T. M., Stitt, T. N., Yancopoulos, G. D., and Glass, D. J. (2001) Identification of ubiquitin ligases required for skeletal muscle atrophy. *Science* **294,** 1704–1708
2. Gomes, M. D., Lecker, S. H., Jagoe, R. T., Navon, A., and Goldberg, A. L. (2001) Atrogin-1, a muscle-specific F-box protein highly expressed during muscle atrophy. *Proc. Natl. Acad. Sci. U.S.A.* **98,** 14440–14445
3. Ponting, C. P., Phillips, C., Davies, K. E., and Blake, D. J. (1997) PDZ domains: targeting signalling molecules to sub-membranous sites. *Bioessays* **19,** 469–479
4. Harrison, S. C. (1996) Peptide-surface association: the case of PDZ and PTB domains. *Cell* **86,** 341–343
5. Julie, L. C., Sabrina, B. P., Marie-Pierre, L., and Leibovitch, S. A. (2012) Identification of essential sequences for cellular localization in the muscle-specific ubiquitin E3 ligase MAFbx/Atrogin 1. *FEBS Lett.* **586,** 362–367
6. Lagirand-Cantaloube, J., Offner, N., Csibi, A., Leibovitch, M. P., Batonnet-Pichon, S., Tintignac, L. A., Segura, C. T., and Leibovitch, S. A. (2008) The initiation factor eIF3-f is a major target for Atrogin1/MAFbx function in skeletal muscle atrophy. *EMBO J.* **27,** 1266–1276
7. Tintignac, L. A., Lagirand, J., Batonnet, S., Sirri, V., Leibovitch, M. P., and Leibovitch, S. A. (2005) Degradation of MyoD mediated by the SCF (MAFbx) ubiquitin ligase. *J. Biol. Chem.* **280,** 2847–2856
8. Xie, P., Guo, S., Fan, Y., Zhang, H., Gu, D., and Li, H. (2009) Atrogin-1/MAFbx enhances simulated ischemia/reperfusion-induced apoptosis in cardiomyocytes through degradation of MAPK phosphatase-1 and sustained JNK activation. *J. Biol. Chem.* **284,** 5488–5496
9. Chou, J. L., Su, H. Y., Chen, L. Y., Liao, Y. P., Hartman-Frey, C., Lai, Y. H., Yang, H. W., Deatherage, D. E., Kuo, C. T., Huang, Y. W., Yan, P. S., Hsiao, S. H., Tai, C. K., Lin, H. J. L., Davuluri, R. V., Chao, T. K., Nephew, K. P., Huang, T. H. M., Lai, H. C., and Chan, M. W. Y. (2010) Promoter hypermethylation of FBXO32, a novel TGF-β/SMAD4 target gene and tumor suppressor, is associated with poor prognosis in human ovarian cancer. *Lab. Invest.* **90,** 414–425
10. Guo, W., Zhang, M., Shen, S., Guo, Y., Kuang, G., Yang, Z., and Dong, Z. (2014) Aberrant methylation and decreased expression of the TGF-β/Smad target gene FBXO32 in esophageal squamous cell carcinoma. *Cancer* **120,** 2412–2423
11. Ciarapica, R., De Salvo, M., Carcarino, E., Bracaglia, G., Adesso, L., Leoncini, P. P., Dall'Agnese, A., Walters, Z. S., Verginelli, F., De Sio, L., Boldrini, R., Inserra, A., Bisogno, G., Rosolen, A., Alaggio, R., Ferrari, A., Collini, P., Locatelli, M., Stifani, S., Screpanti, I., Rutella, S., Yu, Q., Marquez, V. E., Shipley, J., Valente, S., Mai, A., Miele, L., Puri, P. L., Locatelli, F., Palacios, D., and Rota, R. (2014) The Polycomb group (PcG) protein EZH2 supports the survival of PAX3-FOXO1 alveolar rhabdomyosarcoma by repressing FBXO32 (Atrogin1/MAFbx). *Oncogene* **33,** 4173–4184
12. Reed, S. A., Sandesara, P. B., Senf, S. M., and Judge, A. R. (2012) Inhibition of FoxO transcriptional activity prevents muscle fiber atrophy during cachexia and induces hypertrophy. *FASEB J.* **26,** 987–1000
13. Zhang, G., Jin, B., and Li, Y. P. (2011) C/EBPβ mediates tumour-induced ubiquitin ligase atrogin1/MAFbx upregulation and muscle wasting. *EMBO J.* **30,** 4323–4335
14. Farrell, A. S., and Sears, R. C. (2014) MYC degradation. *Cold Spring Harb. Perspect. Med.* 10.1101/cshperspect.a014365
15. Yada, M., Hatakeyama, S., Kamura, T., Nishiyama, M., Tsunematsu, R., Imaki, H., Ishida, N., Okumura, F., Nakayama, K., and Nakayama, K. I. (2004) Phosphorylation-dependent degradation of c-Myc is mediated by the F-box protein Fbw7. *EMBO J.* **23,** 2116–2125
16. Welcker, M., Orian, A., Jin, J., Grim, J. E., Harper, J. W., Eisenman, R. N., and Clurman, B. E. (2004) The Fbw7 tumor suppressor regulates glycogen synthase kinase 3 phosphorylation-dependent c-Myc protein degradation. *Proc. Natl. Acad. Sci. U.S.A.* **101,** 9085–9090
17. Kim, S. Y., Herbst, A., Tworkowski, K. A., Salghetti, S. E., and Tansey, W. P. (2003) Skp2 regulates Myc protein stability and activity. *Mol. Cell* **11,** 1177–1188
18. von der Lehr, N., Johansson, S., Wu, S., Bahram, F., Castell, A., Cetinkaya, C., Hydbring, P., Weidung, I., Nakayama, K., Nakayama, K. I., Söderberg, O., Kerppola, T. K., and Larsson, L. G. (2003) The F-box protein Skp2 participates in c-Myc proteosomal degradation and acts as a cofactor for c-Myc-regulated transcription. *Mol. Cell* **11,** 1189–1200
19. Popov, N., Schülein, C., Jaenicke, L. A., and Eilers, M. (2010) Ubiquitylation of the amino terminus of Myc by SCF(β-TrCP) antagonizes SCF(Fbw7)-mediated turnover. *Nat. Cell Biol.* **12,** 973–981
20. Persson, H., Gray, H. E., Godeau, F., Braunhut, S., and Bellvé, A. R. (1986) Multiple growth-associated nuclear proteins immunoprecipitated by antisera raised against human c-Myc peptide antigens. *Mol. Cell Biol.* **6,** 942–949
21. Rabbitts, P. H., Watson, J. V., Lamond, A., Forster, A., Stinson, M. A., Evan,

G., Fischer, W., Atherton, E., Sheppard, R., and Rabbitts, T. H. (1985) Metabolism of c-*myc* gene products: c-*myc* messenger RNA and protein expression in the cell cycle. *EMBO J.* **4,** 2009–2015
22. Dean, M., Levine, R. A., Ran, W., Kindy, M. S., Sonenshein, G. E., and Campisi, J. (1986) Regulation of c-*myc* transcription and messenger RNA abundance by serum growth factors and cell contact. *J. Biol. Chem.* **261,** 9161–9166
23. Waters, C. M., Littlewood, T. D., Hancock, D. C., Moore, J. P., and Evan, G. I. (1991) c-Myc protein expression in untransformed fibroblasts. *Oncogene* **6,** 797–805
24. Stitt, T. N., Drujan, D., Clarke, B. A., Panaro, F., Timofeyva, Y., Kline, W. O., Gonzalez, M., Yancopoulos, G. D., and Glass, D. J. (2004) The IGF-1/PI3K/Akt pathway prevents short article expression of muscle atrophy-induced ubiquitin ligases by inhibiting FOXO transcription factors. *Mol. Cell* **14,** 395–403
25. Ferber, E. C., Peck, B., Delpuech, O., Bell, G. P., East, P., and Schulze, A. (2012) FOXO3a regulates reactive oxygen metabolism by inhibiting mitochondrial gene expression. *Cell Death Differ.* **19,** 968–979
26. Delpuech, O., Griffiths, B., East, P., Essafi, A., Lam, E. W. F., Burgering, B., Downward, J., and Schulze, A. (2007) Induction of Mxi1-SR α by FOXO3a contributes to repression of Myc-dependent gene expression. *Mol. Cell Biol.* **27,** 4917–4930
27. Sandri, M., Sandri, C., Gilbert, A., Skurk, C., Calabria, E., Picard, A., Walsh, K., Schiaffino, S., Lecker, S. H., and Goldberg, A. L. (2004) Foxo transcription factors induce the atrophy-related ubiquitin ligase atrogin-1 and cause skeletal muscle atrophy. *Cell* **117,** 399–412
28. Sears, R., Ohtani, K., and Nevins, J. R. (1997) Identification of positively and negatively acting elements regulating expression of the E2F2 gene in response to cell growth signals. *Mol. Cell Biol.* **17,** 5227–5235
29. Feng, X., Liu, X., Zhang, W., and Xiao, W. (2011) p53 directly suppresses BNIP3 expression to protect against hypoxia-induced cell death. *EMBO J.* **30,** 3397–3415
30. Wang, J., Zhang, W., Ji, W., Liu, X., Ouyang, G., and Xiao, W. (2014) The von Hippel-Lindau protein suppresses androgen receptor activity. *Mol. Endocrinol.* **28,** 239–248
31. Chen, Z., Liu, X., Mei, Z., Wang, Z., and Xiao, W. (2014) EAF2 suppresses hypoxia-induced factor 1α transcriptional activity by disrupting its interaction with coactivator CBP/p300. *Mol. Cell. Biol.* **34,** 1085–1099
32. Hoang, A. T., Lutterbach, B., Lewis, B. C., Yano, T., Chou, T. Y., Barrett, J. F., Raffeld, M., Hann, S. R., and Dang, C. V. (1995) A link between increased transforming activity of lymphoma-derived Myc mutant alleles, their defective regulation by P107, and altered phosphorylation of the c-Myc transactivation domain. *Mol. Cell Biol.* **15,** 4031–4042
33. Noguchi, K., Kitanaka, C., Yamana, H., Kokubu, A., Mochizuki, T., and Kuchino, Y. (1999) Regulation of c-Myc through phosphorylation at Ser-62 and Ser-71 by c-Jun N-terminal kinase. *J. Biol. Chem.* **274,** 32580–32587
34. Sanchez-Arévalo Lobo, V. J., Doni, M., Verrecchia, A., Sanulli, S., Fagà, G., Piontini, A., Bianchi, M., Conacci-Sorrell, M., Mazzarol, G., Peg, V., Losa, J. H., Ronchi, P., Ponzoni, M., Eisenman, R. N., Doglioni, C., and Amati, B. (2013) Dual regulation of Myc by Abl. *Oncogene* **32,** 5261–5271
35. Bartholomeusz, G., Talpaz, M., Bornmann, W., Kong, L. Y., and Donato, N. J. (2007) Degrasyn activates proteasomal-dependent degradation of c-Myc. *Cancer Res.* **67,** 3912–3918
36. Huang, Z., Traugh, J. A., and Bishop, J. M. (2004) Negative control of the Myc protein by the stress-responsive kinase Pak2. *Mol. Cell Biol.* **24,** 1582–1594
37. Meyer, N., and Penn, L. Z. (2008) Reflecting on 25 years with MYC. *Nat. Rev. Cancer* **8,** 976–990
38. Lahav, G., Rosenfeld, N., Sigal, A., Geva-Zatorsky, N., Levine, A. J., Elowitz, M. B., and Alon, U. (2004) Dynamics of the p53-Mdm2 feedback loop in individual cells. *Nat. Genet.* **36,** 147–150
39. Ikeda, F., and Dikic, I. (2008) Atypical ubiquitin chains: new molecular signals: "Protein modifications: Beyond the usual suspects" review series. *EMBO Rep.* **9,** 536–542
40. Kulathu, Y., and Komander, D. (2012) Atypical ubiquitylation: the unexplored world of polyubiquitin beyond Lys48 and Lys63 linkages. *Nat. Rev. Mol. Cell Biol.* **13,** 508–523
41. Bretones, G., Acosta, J. C., Caraballo, J. M., Ferrándiz, N., Gómez-Casares, M. T., Albajar, M., Blanco, R., Ruiz, P., Hung, W. C., Albero, M. P., Perez-Roger, I., and León, J. (2011) SKP2 oncogene is a direct MYC target gene and MYC down-regulates p27(KIP1) through SKP2 in human leukemia cells. *J. Biol. Chem.* **286,** 9815–9825
42. Barsyte-Lovejoy, D., Mao, D. Y. L., and Penn, L. Z. (2004) c-Myc represses the proximal promoters of GADD45α and GADD153 by a post-RNA polymerase II recruitment mechanism. *Oncogene* **23,** 3481–3486
43. Leone, G., Sears, R., Huang, E., Rempel, R., Nuckolls, F., Park, C. H., Giangrande, P., Wu, L., Saavedra, H. I., Field, S. J., Thompson, M. A., Yang, H., Fujiwara, Y., Greenberg, M. E., Orkin, S., Smith, C., and Nevins, J. R. (2001) Myc requires distinct E2F activities to induce S phase and apoptosis. *Mol. Cell* **8,** 105–113
44. Amati, B., Brooks, M. W., Levy, N., Littlewood, T. D., Evan, G. I., and Land, H. (1993) Oncogenic activity of the c-Myc protein requires dimerization with Max. *Cell* **72,** 233–245
45. Kipreos, E. T., and Pagano, M. (2000) The F-box protein family. *Genome Biol.* **1,** REVIEWS3002
46. Baltgalvis, K. A., Berger, F. G., Peña, M. M. O., Davis, J. M., White, J. P., and Carson, J. A. (2009) Muscle wasting and interleukin-6-induced atrogin-I expression in the cachectic Apc (Min/+) mouse. *Pflugers Arch. Eur. J. Physiol.* **457,** 989–1001
47. Tan, J., Yang, X., Zhuang, L., Jiang, X., Chen, W., Lee, P. L., Karuturi, R. K. M., Tan, P. B. O., Liu, E. T., and Yu, Q. (2007) Pharmacologic disruption of polycomb-repressive complex 2-mediated gene repression selectively induces apoptosis in cancer cells. *Genes Dev.* **21,** 1050–1063
48. Tansey, W. P. (2014) Mammalian MYC proteins and cancer. *New J. Sci.* **2014,** 1–27